



Anionic congo red dye removal from aqueous medium using Turkey tail (*Trametes versicolor*) fungal biomass: adsorption kinetics, isotherms, thermodynamics, reusability, and characterization

Venkata Subbaiah Munagapati , Hsin-Yu Wen , Jet-Chau Wen , Yuvaraja Gutha , Zhong Tian , Guda Mallikarjuna Reddy & Jarem Raul Garcia

To cite this article: Venkata Subbaiah Munagapati , Hsin-Yu Wen , Jet-Chau Wen , Yuvaraja Gutha , Zhong Tian , Guda Mallikarjuna Reddy & Jarem Raul Garcia (2020): Anionic congo red dye removal from aqueous medium using Turkey tail (*Trametes versicolor*) fungal biomass: adsorption kinetics, isotherms, thermodynamics, reusability, and characterization, Journal of Dispersion Science and Technology, DOI: [10.1080/01932691.2020.1789468](https://doi.org/10.1080/01932691.2020.1789468)

To link to this article: <https://doi.org/10.1080/01932691.2020.1789468>



Published online: 07 Jul 2020.



Submit your article to this journal [↗](#)



View related articles [↗](#)



View Crossmark data [↗](#)



Anionic congo red dye removal from aqueous medium using Turkey tail (*Trametes versicolor*) fungal biomass: adsorption kinetics, isotherms, thermodynamics, reusability, and characterization

Venkata Subbaiah Munagapati^a, Hsin-Yu Wen^b, Jet-Chau Wen^{a,c}, Yuvaraja Gutha^d, Zhong Tian^e, Guda Mallikarjuna Reddy^{f,g}, and Jarem Raul Garcia^g

^aResearch Centre for Soil & Water Resources and Natural Disaster Prevention (SWAN), National Yunlin University of Science & Technology, Douliou, Yunlin, Taiwan, ROC; ^bDepartment of Pathology, West China Hospital, Sichuan University, Chengdu, PR China; ^cDepartment and Graduate School of Safety and Environment Engineering, National Yunlin University of Science & Technology, Douliou, Yunlin, Taiwan, ROC; ^dSchool of Civil Engineering, Guangzhou University, Guangzhou, PR China; ^eState Key Laboratory of Hydraulics and Mountain River Engineering, Sichuan University, Chengdu, PR China; ^fChemical Engineering Institute, Ural Federal University, Yekaterinburg, Russian Federation; ^gDepartment of Chemistry, State University of Ponta Grossa, Ponta Grossa, Brazil

ABSTRACT

Turkey tail (*Trametes versicolor*), cheap fungal biomass (TTFB), was used for the adsorption of CR from aqueous medium. Batch studies conducted to study the effect of pH (2.0–10.0), agitation speed (50–400 rpm), contact time (0–180 min), adsorbate concentration (300 and 500 mg/L), and temperature (303–333 K). TTFB characterized by FTIR, BET, SEM, and pH_{pzc}. The maximum mono-layer adsorption capacities of CR on TTFB were 318.1, 368.4, 394.8, and 415.7 mg/g at 303, 313, 323, and 333 K, respectively. The adsorption of CR was pH-dependent and maximum adsorption attained at pH 2.0 at all temperatures. Adsorption kinetic data evaluated by using the PFO and PSO non-linear equations. The kinetic data perfectly illustrated by the PSO model with $R^2 > 9935$. Langmuir, Freundlich, D-R, and Temkin nonlinear isotherms applied for the experimental data, and it observed that the experimental data well fitted and found to be in good agreement with the Langmuir model ($R^2 > 0.9961$) as compared with another three models. The values of ΔG° (–3.4159 to –6.1149 kJ/mol), ΔH° (23.2 kJ/mol), and ΔS° (0.088 kJ/mol K) revealed that the adsorption process was spontaneous, feasible and endothermic ($\Delta G^\circ < 0$, $\Delta S^\circ > 0$, and $\Delta H^\circ > 0$). The regeneration experiments indicated that the TTFB could successfully retain CR, even after five consecutive adsorption-desorption cycles. The binding of CR onto the TTFB surface was through electrostatic interactions. Therefore, TTFB considered as highly recyclable and efficient adsorbent material for CR as it can easily separate from the aqueous phase.

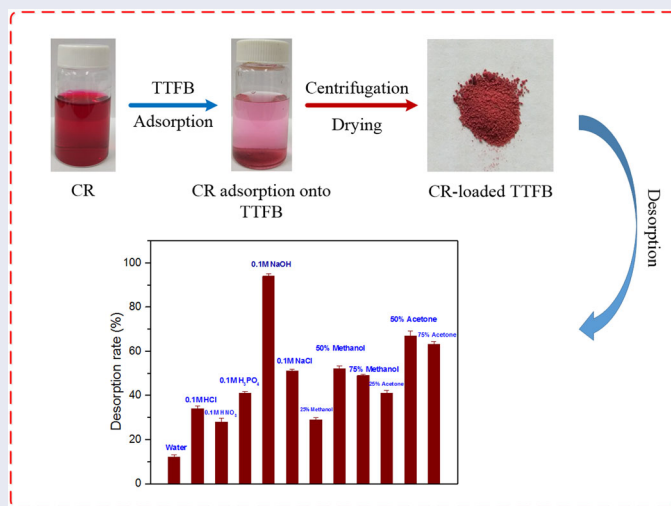
ARTICLE HISTORY

Received 2 February 2020
Accepted 13 June 2020

KEYWORDS

Adsorption; congo red; isotherms; kinetics; thermodynamics

GRAPHICAL ABSTRACT



Introduction

For the existence of living species, water is an essential ecological resource available on the earth. Amid, the purity of water is another critical aspect to be accounted for. The rapid surge in technological advancements, industrialization, urbanization severely affected the purity of the water bodies. Among the various contaminants, the toxic and deficient degradable organic dyes are the prime pollutants of the water.^[1,2] Dyes bearing azo groups ($R_1-N=N-R_2$) are considered as one of the most important and more exciting sub-classes of organic dyes and could be cationic (basic), anionic (reactive, acid, and direct), and nonionic (disperse and vat). Congo red is an anionic diazo dye generally used in rubber, wood pulp, plastic, printing, dyeing, biological stain, and textile industries. The CR has been a significant component in the industrial discharge. Due to its high-water solubility, it is posing a significant threat to aquatic organisms as well. In the anaerobic conditions, this dye is undergoing chemical degradation leading to the formation of toxic aromatic amines, which considered to be carcinogenic and teratogenic.^[1] Therefore, it is highly essential to remove CR from contaminated water before getting discharged to the aquatic streams.

Different treatment methods such as biological, chemical, and physical conditions have been developed since decades to remove dyes from aqueous solutions such as liquid membrane separation,^[3] oxidation,^[4] photodegradation,^[5] coagulation/flocculation,^[6] ozonation,^[7] incineration,^[8] and adsorption^[9–13] but most of these techniques are beginning to prove insufficient for simple and effective treatment; also they are costly. It is essential to think about useful methods and inexpensive. Adsorption is recognized to be one of the most competitive ways due to the exhibition of several advantages such as smooth operation, potentially low-cost, high efficiency, zero secondary pollution, simplicity of design, and the broad availability of the adsorbent materials. Therefore, the search for the development of new adsorbents with high surface area, inexpensive, sustainable, higher sorption capacity, and regeneration capability is the critical area to focus in recent years. Different types of adsorbents such as garlic straw,^[14] powdered orange peel,^[15] green adsorbents,^[16] wood apple shell,^[17] breadnut peel,^[18] grapefruit peel,^[19] barberry stem,^[20] *salix babylonica* (weeping willow) leaves powder,^[21] walnut shells powder,^[22] rice husk,^[23] sunflower stalk,^[24] activated carbon,^[25] activated carbon fiber (coconut husk),^[26–28] *ficus auriculata* leaves powder,^[29] *strychnos nux-vomica* shell,^[30] *colocasia esculenta* leaves,^[31] and *swietenia mahagoni* shell^[32] have been utilized for the removal of dyes and metals from wastewater. In the present work, the aim was to remove CR from aqueous phase using a TTFB with the adsorption technique.

Several studies have revealed the excellent adsorption capacity of various pollutants from aqueous solution using biomasses, like bacteria, algae, fungi, yeasts, seaweeds, and other materials.^[33] Additionally, there is no risk of providing nutrients in the case of dead biomass over live biomass. In particular, the presence of chitin, glucans, and proteins, fungal biomasses in some fungal biomasses, made them

potential adsorbents. The functional groups present in the cell wall like amine, hydroxyl, thiol, phosphate, and carbonyl are capable of binding dye molecules.^[34,35] Fungal biomass could be a useful adsorbent of dyes. Various types of fungal biomass have been studied as adsorbents to eliminate dyes from contaminated water such as *Aspergillus niger*,^[36] *Aspergillus flavus*,^[37] *Aspergillus alliaceus*,^[38] *Penicillium ochrochloron*,^[39] *Rhizopus arrhizus*,^[40] *Penicillium restrictum*,^[41] and *Aspergillus fumigatus*.^[42] The fungal species *Trametes versicolor*, commonly names Turkey tail, is a widely growing lignicolous fungus on oak, prunus trees, as well as the fir, pine conifers. The basidiums of these fungi could appear mostly on trees stubs and trunks. The TTFB was chosen as an adsorbent in this study as it is natural, readily available, and thus inexpensive material for the removal of CR from aqueous medium.

The influence of various critical parameters including pH of the solution, agitation speed, adsorbate concentration, contact time, and temperature were thoroughly investigated. The TTFB characterized by FTIR, SEM, BET, and pH_{pzc} . The capability of TTFB for CR adsorption evaluated by applying various isotherms, kinetics, and thermodynamic parameters. Using desorption and regeneration data the potential of TTFB for CR was determined.

Materials and methods

Materials

All chemicals and reagents used in the present study were of analytical grade and requires no further purification. Congo red (CR), reactive black 5 (RB5), methyl orange (MO), reactive red 120 (RR120), direct red 23 (DR23), malachite green (MG), and methylene blue (MB) were obtained from Sigma Aldrich, India. The molecular structure of the used dyes is tabulated in Table 1. Double de-ionized water was used to prepare all solutions.

Preparation of adsorbent and adsorbate

Turkey tail (*Trametes versicolor*) fungal biomass was used as an adsorbent material for the adsorption of CR. TTFB was collected from Tirumala Tirupati Hills (Andhra Pradesh, India), dried under sunlight, and ground into a fine powder. The resultant TTFB powder is thoroughly washed several times with double de-ionized water and dried at 353 K for 24 h. Further the powder is, boiled in double de-ionized water by changing the water frequently until the water becomes colorless, to ensure the removal of water-soluble color substances. The resulting TTFB powder was oven-dried at 353 K for 24 h, and sieved to 35 (0.5 mm) mesh sieve and stored in a desiccator for the further use. An aqueous stock solution of CR with a concentration of 1,000 mg/L was prepared and further diluted to the necessary concentrations.

Table 1. Molecular structure and characteristics of the used dyes.

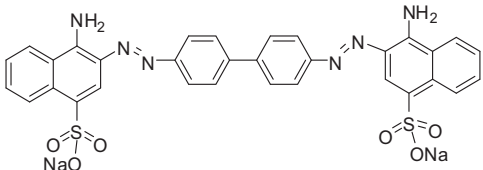
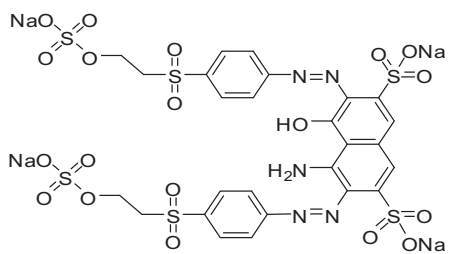
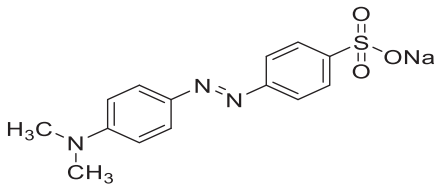
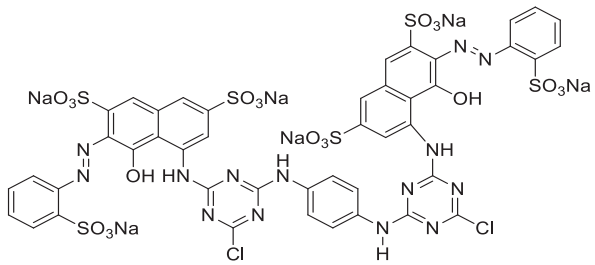
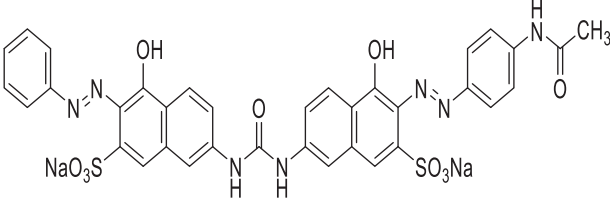
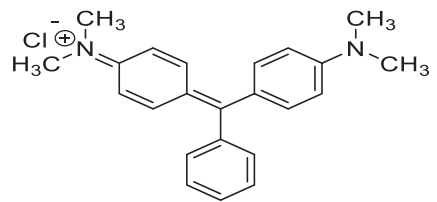
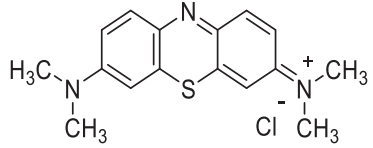
Dye	Chemical structure	λ_{\max} (nm)	Molecular weight (g/mol)
CR		497	696.66
RB5		597	991.78
MO		464	327.33
RR120		515	1469.98
DR23		507	813.72
MG		617	364.91
MB		665	319.85

Table 2. Langmuir, Freundlich, D-R, and Temkin isotherm parameters for the CR onto TTFB.

Temp.	Langmuir				Freundlich				Dubinin-Radushkevich				Temkin				
	q_m (mg/g)	k_L (L/mg)	R^2	χ^2	K_f (mg/g)	n	R^2	χ^2	q_m (mg/g)	K	E	R^2	χ^2	b (kJ/mol)	α (L/mg)	R^2	χ^2
303	318.1	0.0169	0.9974	31.8	49.28	3.53	0.9463	136.1	265.1	0.0449	3.3	0.8383	263.1	0.040	0.2072	0.9568	95.3
313	368.4	0.0179	0.9967	44.1	55.27	3.41	0.9355	153.4	306.4	0.0406	3.5	0.8627	243.8	0.035	0.2114	0.9623	85.6
323	394.8	0.0222	0.9961	56.3	67.41	3.59	0.9296	170.8	328.2	0.0312	4.0	0.8297	287.6	0.036	0.3013	0.9571	93.1
333	415.7	0.0231	0.9969	61.3	78.86	3.86	0.9706	119.2	354.1	0.0354	3.8	0.7928	387.2	0.042	0.6457	0.9766	78.4

Characterization of the TTFB

To understand the adsorption mechanism of CR onto TTFB, the adsorbent was characterized by FTIR (Nicolet IS10, Thermo Scientific, USA) before and after the adsorption process. FTIR spectrum was recorded by using pellets made of KBr with spectral scanning range of 400–4000 cm^{-1} . The BET surface area of TTFB was measured from N_2 adsorption/desorption isotherms at 77 K (BELSORP, BEL Japan) after degassing the adsorbent at 323 K for 12 h in an inert atmosphere. In addition, the total pore volume and mean pore diameter was measured by the BJH method. The surface morphology of TTFB (before and after CR adsorption) was observed using a scanning electron microscope (JEOL, JSM-7600F, Japan) under vacuum and 25.0 kV using tungsten filament. The TTFB samples were gold coated using the sputter coater to form a thin layer. The pH_{pzc} of TTFB was determined by the solid addition method^[43] using 0.01 M NaCl solution as the electrolyte. The experiments carried out in a series of 50 mL falcon tubes, each containing 30 mL of 0.01 M NaCl. The initial pH (pH_i) of these solutions were adjusted in the range of 2.0–10.0 by adding either HCl or NaOH (0.1 M). The adsorbent (0.05 g) was added to each tube and the suspensions were placed in the incubator was for 24 h under specified conditions of agitation speed 250 rpm, temperature 303 K, and the final pH of suspension (pH_f) was determined. The pH_{pzc} was obtained from the plot of ($\text{pH}_i - \text{pH}_f$) against the pH_i .

Batch adsorption experiments

Adsorption behavior of CR onto TTFB was determined using Batch studies. The pH experiments were performed by mixing 0.05 g of TTFB in 30 mL of CR solution with an initial concentration of 300 mg/L into 50 mL polypropylene tubes. The pH is adjusted in the range of 2.0–10.0 adding the appropriate volume of acid and alkaline solution, that is, HCl or NaOH (0.1 M). The resultant pH values of the CR solutions were measured by pH meter (Orion 4 star, Thermo Scientific, USA). Kinetic experiments were carried out by adding 0.05 g of TTFB to 30 mL of CR solution (300 and 500 mg/L), and the adsorption processes carried out in a shaker at 298 K with shaking at 250 rpm, but with various time intervals (0–180 min). Adsorption isotherm experiments conducted by adding 0.05 g of TTFB to 30 mL different initial concentrations of CR solution (100, 200, 300, 400, 500, 700, and 1000 mg/L) and the adsorption process carried out in a shaker at four different temperatures (303, 313, 323, and 333 K) at 250 rpm for 120 min. The effect of temperature also investigated by the addition of TTFB (0.05 g) to 30 mL of CR dye (300 mg/L) solution. The experiments conducted for 120 min for different temperatures (303–333 K).

After attaining the equilibrium time, the solution samples were centrifuged at 5,000 rpm for 15 min to separate the adsorbent and the remaining CR concentration was measured using UV/Vis spectrophotometer (JASCO V-750, Japan) at a wavelength of 497 nm. Equation (1) was used to calculate the amount of CR adsorbed onto TTFB.

$$q_e = \frac{(C_o - C_e)V}{M} \quad (1)$$

Desorption and reusability studies

The desorption experiments were carried out with different desorbing eluents. The experiments conducted by adding 0.1 g of TTFB in 30 mL of 300 mg/L concentration of CR within 120 min at pH 2.0 and 303 K. The free adsorbent was washed with distilled water several times to eliminate the traces of CR. The CR-loaded TTFB was agitated separately, with 30 mL of the various desorbing eluents. After desorption, the solutions were filtered, and the amount of CR desorbed was measured. The TTFB was another time used for the adsorption of CR, and the all process of adsorption-desorption of TTFB was repeated for five successive cycles. The desorption efficiency was calculated by the following Eq. (2):

$$\text{Desorption efficiency} = \frac{\text{Amount of CR desorbed}}{\text{Amount of CR adsorbed}} \times 100 \quad (2)$$

χ^2 analysis

Nonlinear χ^2 statistical error analysis is most appropriate to interpret adsorption data. The lower χ^2 value implies the isotherm model is similar to the experimental data. The advantage of the χ^2 analysis is that all isotherms can be compared in the same horizontal and longitudinal coordinates. The χ^2 values of each isotherm models were shown in Table 2. The equivalent mathematical statement of χ^2 analysis is as follows:

$$\chi^2 = \sum_{i=1}^n \left(\frac{(q_e - q_{e,m})^2}{q_{e,m}} \right) \quad (3)$$

Results and discussion

Characterization

FTIR spectroscopy is an important technique to recognize and verify the specific functional groups present on the surface of TTFB, that helps to identify the active adsorption sites for CR dye molecule. Figure 1 shows the FT-IR spectrum for

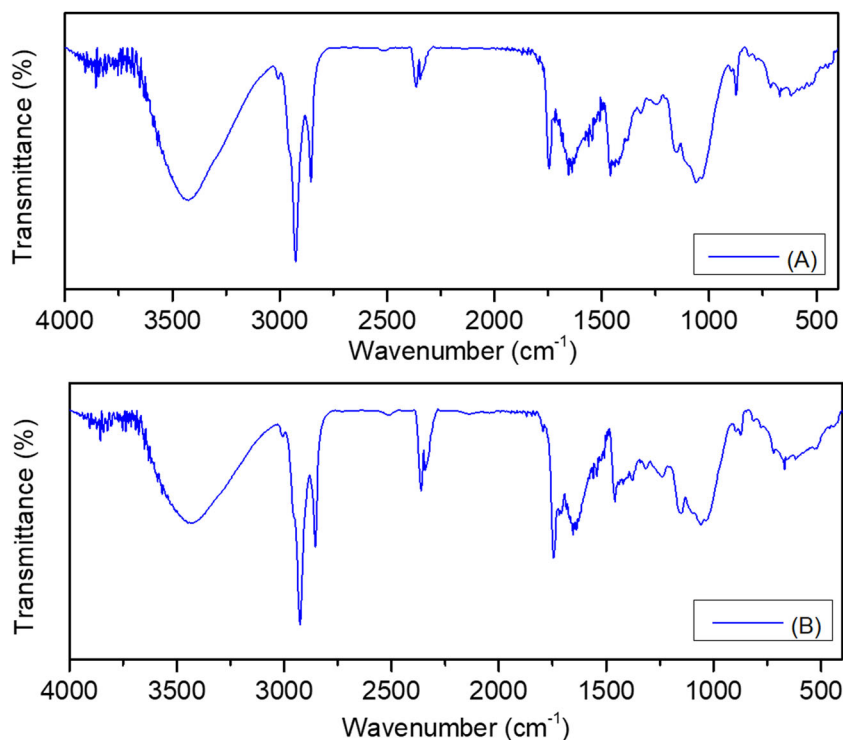


Figure 1. FTIR images of (A) TTFB and (B) CR-loaded TTFB.

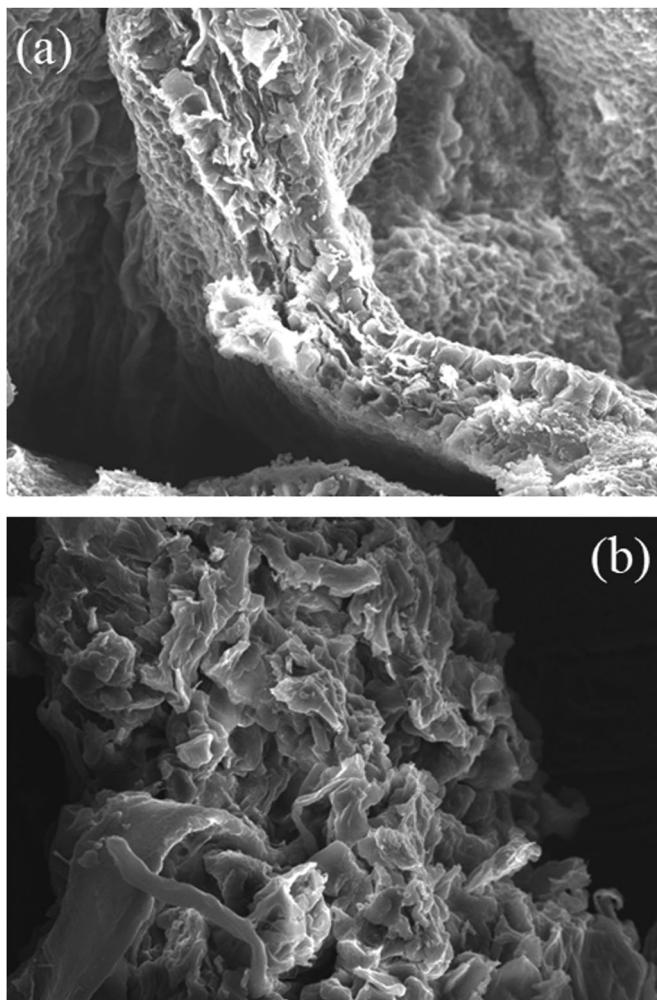


Figure 2. SEM images of (A) TTFB and (B) CR-loaded TTFB.

TTFB before and after the adsorption of CR. The spectrum of TTFB (Figure 1A) showed distinct major peaks at 3428, 2926, 2854, 1739, 1654, 1561, 1460, 1318, 1244, 1148, 1059, and 873 cm^{-1} . The strong band at 3428 cm^{-1} is mainly due to the stretching vibration of O-H bonds in a hydroxyl group. The sharp peaks at 2926 and 2854 cm^{-1} may be attributed to the C-H stretching of the alkyl groups. The peak at 1739 cm^{-1} ascribed to the C=O stretching vibration of the carbonyl group. The adsorption peaks about 1654 and 1561 cm^{-1} were assigned to the C=O and N-H bonds of carboxyl or amide groups. The band at 1460 cm^{-1} ascribed to the bending OH vibration of hydroxyl groups. The peak at 1318 cm^{-1} may be attributed to O-H bending of alcohol and C-H bending of the alkyl group. The band at 1244 cm^{-1} represents the C-H stretching vibrations. The two peaks at 1148 and 1059 cm^{-1} corresponds to the C-O and C=O groups, respectively. The peak at 873 cm^{-1} refers to out of plane bending vibration of aromatic compounds. The peaks at 3436, 2921, 2849, 1744, 1656, 1558, 1454, 1322, 1236, 1153, 1063, and 862 cm^{-1} were observed in the FTIR spectra of TTFB after the adsorption (Figure 1B). The surface of the TTFB adsorbent revealed peaks are slightly shifted from their initial positions after the adsorption of CR, demonstrating the contribution of the respective functional groups during the sorption process.

The fundamental physical properties like particle shape, porosity, and appropriate size distribution of the sorbent and surface morphology of the sorbent surface are the important parameters and characterized by SEM analysis. Figure 2 displays SEM micrographs for TTFB before and after the adsorption of CR. A considerable number of heterogeneous pores were observed on the TTFB surface, bringing the possibility for dyes to be trapped and adsorbed onto these pores (Figure 2A). After CR adsorption, the surface of

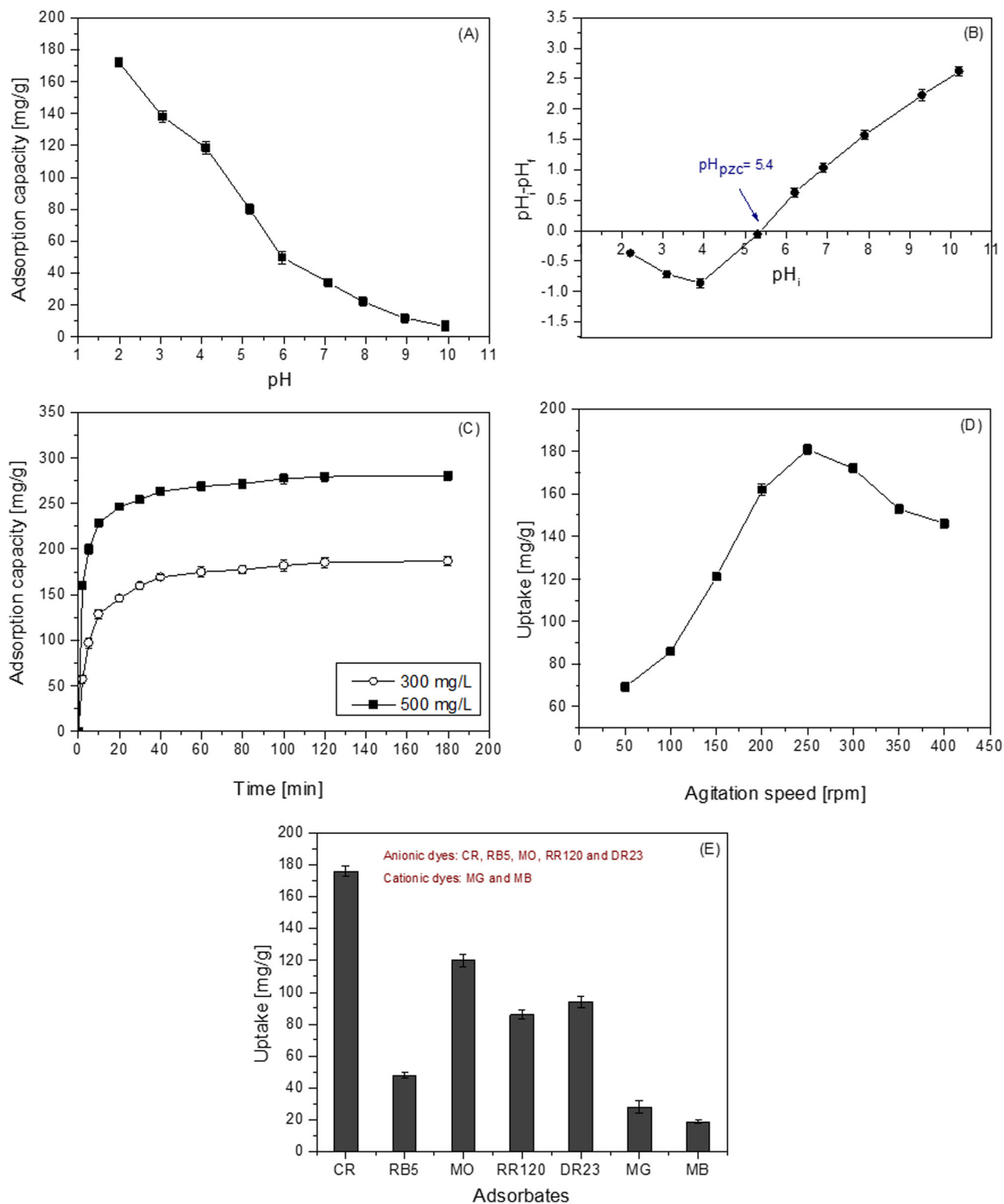


Figure 3. (A) Effect of pH on the adsorption of CR onto TTFB, (B) Point of zero charge (pH_{pzc}) of TTFB, (C) Effect of contact time on the adsorption of CR onto TTFB, (D) Effect of agitation speed on the adsorption of CR onto TTFB, and (E) Adsorption capacities of TTFB toward various anionic and cationic dyes.

TTFM completely pored was covered with CR dye, confirming the adsorption of CR onto TTFB (Figure 2B).

The surface area and porosity (mean pore diameter and total pore volume) of the adsorbent contributes a significant portion in the adsorption capacity. The surface area, mean pore diameter, and total pore volume of TTFB measured by BET and BJH methods. It found that the mean pore diameter, total pore volume, and surface area of the TTFB were 23.2 nm,

0.1126 cm^3/g , and 18.6 m^2/g , respectively. These properties increased the CR adsorption possibility onto TTFB.

Effect of pH

The pH solution is one of the most significant factors that could affect the adsorption process by controlling the surface

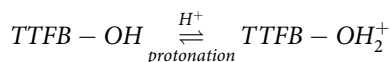
Table 3. Parameters obtained from pseudo-first-order and pseudo-second-order kinetic models for the adsorption of CR onto TTFB.

Adsorbent	Conc. (mg/L)	$q_{e, \text{exp}}$ (mg/g)	Pseudo-first-order model			Pseudo-second-order model		
			$q_{e1, \text{cal}}$ (mg/g)	k_1 (1/min)	R^2	$q_{e2, \text{cal}}$ (mg/g)	k_2 (g/mg min)	R^2
TTFB	300	184.6	174.9	0.1430	0.9707	189.7	0.0011	0.9980
	500	273.8	263.9	0.3571	0.9581	276.4	0.0021	0.9935

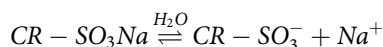
chemistry of adsorbent and the dye solubility. Effect of pH on the CR adsorption onto TTFB was carried out in the pH range of 2.0–10.0 at 303 K. The results related to the effect of pH on the CR adsorption onto TTFB was figured out in Figure 3A. This figure displays that the adsorption capacity of CR decreases from 172.1 to 10.8 mg/g as the pH increases from 2.0 to 10.0. The adsorption of CR firmly depended on pH and the maximum sorption capacity attained at pH 2.0 and pH value of 2.0 was measured to be optimum. From Figure 3B it is seen that the pH_{pzc} of the TTFB was found to be 5.4, which signifies that below this value, the surface of the TTFB was positively charged might be due to protonation and above pH_{pzc} the TTFB was negatively charged. Such high sorption capacity in lower pH values ($\text{pH} < \text{pH}_{\text{pzc}}$) mainly attributed to the possible electrostatic interaction forces exists between the sulfonate groups (-ve charge) of the CR and surface (+ve charge) of the TTFB.

Adsorption mechanism may be as the following equations:

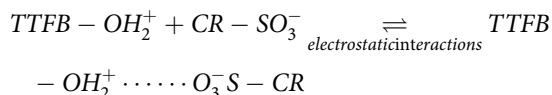
- i. When pH is low, protonation of -OH groups takes place at the surface of TTFB resulted in a positive charge.



- ii. The dissolved CR dye in an aqueous phase behaves as a strong anionic dye by the strong dipole (-ve) polarization of sulfonate groups.



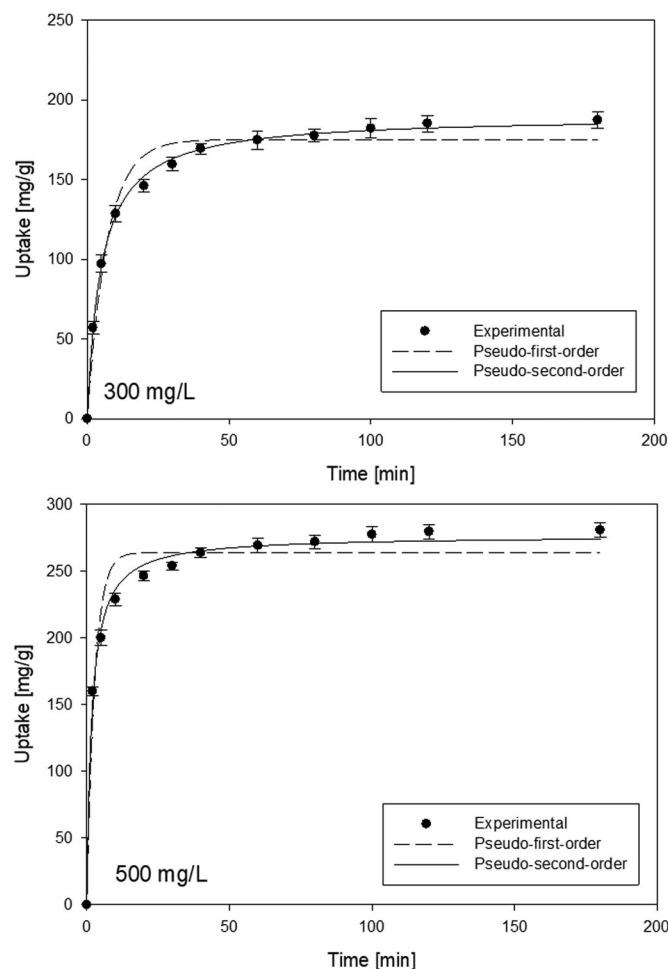
- iii. The adsorption process performed due to electrostatic interactions between the TTFB surface and the CR dye that behaves as anions:



An increase in the solution ($\text{pH} > \text{pH}_{\text{pzc}}$) pH declines the positively charged sites and increases the negatively charged sites. However, this negatively charged surface is not favorable for the adsorption process. Hence, pH 2.0 selected for carrying out further batch adsorption experiments. A similar approach has been found for the adsorption of anionic dyes, as reported in the literature.^[35,44–49]

Effect of contact time

The contact time determines the time required for the adsorption reaction to reach equilibrium. The adsorption capacity of CR by TTFB at different time intervals (0–180 min) at two levels of initial CR dye concentrations


Figure 4. Nonlinear kinetic curves fitted to the pseudo-first-order and pseudo-second-order models.

studied and presented in Figure 3C. It can be seen from Figure 3C; For the two different initial concentrations (300 and 500 mg/L), the adsorption capacity increased until 120 min and there is no appropriate change after 120 min. In the initial stage of the first 30 min, adsorption of CR increased very fast due to the excess availability of free adsorption sites on the TTFB surface. Thus, the optimum equilibrium time of 120 min was considered for further experiments.

Effect of stirring speed

The stirring speed maintains the mobility of the adsorbent and adsorbate and further induces relative mobility for active uptake of dye on the adsorbent surface. Figure 3D shows the effect of stirring speed variation on the adsorption of CR onto TTFB was studied in the range 50–400 rpm, while all other conditions were kept constant. The maximum adsorption efficiency was attained at 250 rpm because

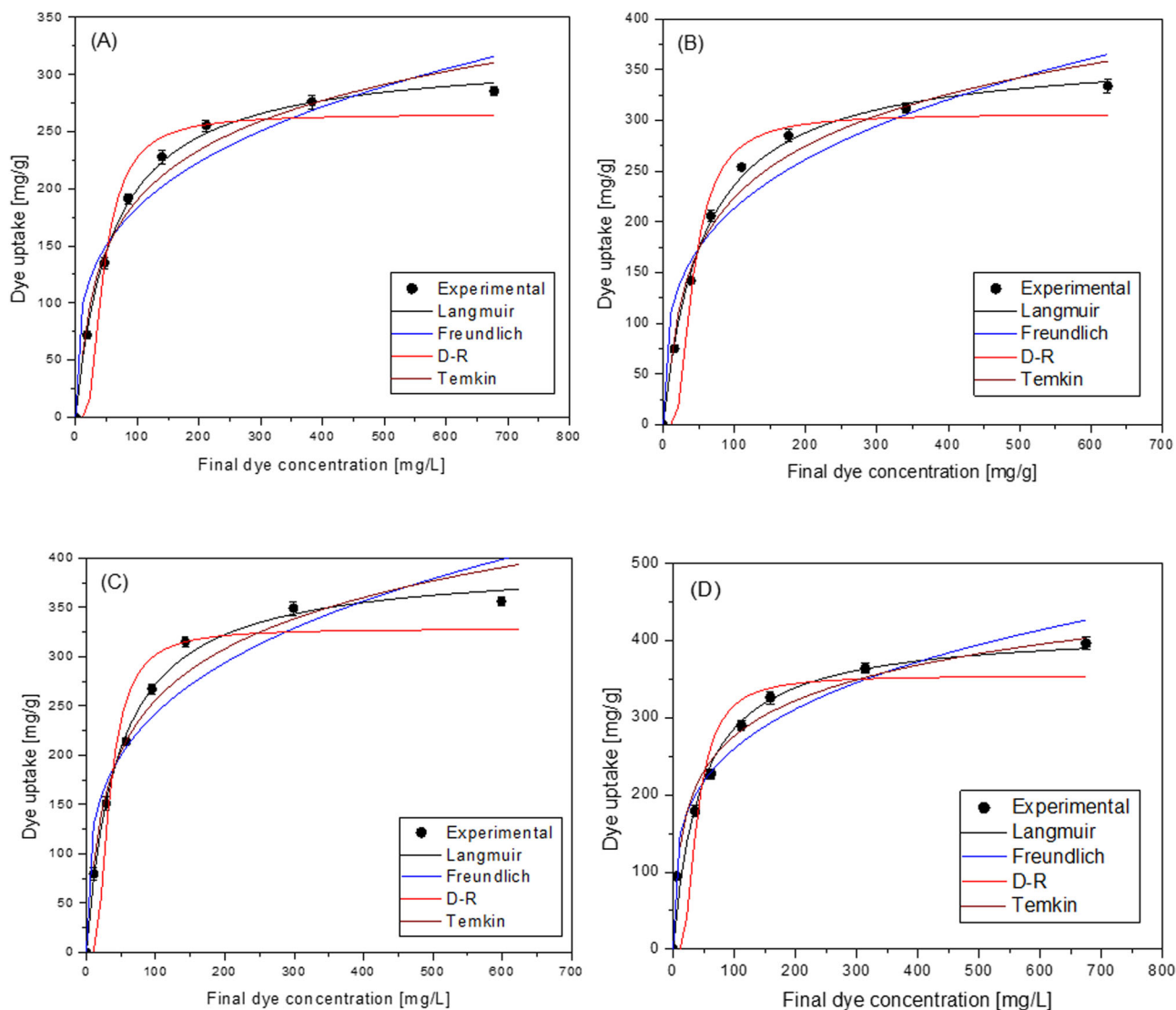


Figure 5. Nonlinear fitting of adsorption isotherms at different temperatures: (A) 303, (B) 313, (C) 323, and (D) 333 K.

of the best homogeneity of the adsorbent suspension. On the contrast, at high speed the suspension is no longer homogeneous because of a vortex phenomenon that makes the CR adsorption difficult. Thus, the optimum stirring speed of 250 rpm is fixed and maintained throughout the study.

Adsorption performance of TTFB toward various dyes

Five types of anionic dyes including CR, RB5, MO, RR120, and DR23 and two types of cationic dyes including MG and MB were selected as representative dyes to estimate the maximum adsorption capacity of TTFB (experimental conditions: adsorbent weight 0.05 g, pH 2.0, agitation speed 250 rpm, adsorbate concentration 300 mg/L (30 mL) and temperature 303 K). As can be seen from Figure 3E, the TTFB is suitable and displays higher sorption capacities for anionic dyes when compared with cationic dyes. For example, its sorption capacity for anionic CR dye can reach 176 mg/g, which is about 6.3- and 9.5-folds of that for cationic MG and MB dyes, respectively. In this study, we have

chosen anionic CR dye as an adsorbate because its adsorption capacity is higher than compared with other anionic and cationic dyes (Figure 3E).

Adsorption kinetics

In industrial applications, adsorption kinetics is of great importance for process design and operation. Kinetic experiments were carried to estimate the impact of initial dye concentration on the dynamic behaviors, by using two various initial levels of 300 and 500 mg/L. The experimental data modeled using the PFO and PSO kinetics is as follows.

PFO model^[50]:

$$q_t = q_{e1}(1 - \exp(-k_1 t)) \quad (4)$$

PSO model^[51]:

$$q_t = \frac{q_{e2}^2 k_2 t}{1 + q_{e2} k_2 t} \quad (5)$$

The experimental values of CR uptake ($q_{e, exp}$), calculated values of CR uptake ($q_{e1, cal}$ and $q_{e2, cal}$), rate constants (k_1

Table 4. Comparison of the maximum adsorption capacities for the removal of CR using various adsorbents.

Adsorbent	q_{max} (mg/g)	pH	References
Spent mushroom	147.1	2.0	[61]
<i>Aspergillus carbonarius</i>	99.01	4.5	[62]
<i>Penicillium glabrum</i>	101.01	4.5	[62]
<i>Penicillium janthinellum</i>	344.83	5.0	[63]
Sugarcane bagasse	38.2	5.0	[64]
Macauba palm cake	32	6.5	[65]
Banana peel powder	164.6	3.0	[66]
Jujuba seed	55.56	2.0	[67]
Corn cob	50	–	[68]
Cattail root	38.79	7.0	[69]
<i>Penicillium</i> sp. YW01	411.53	3.0	[70]
Phoenix dactylifera seeds	61.72	2.0	[71]
<i>Aspergillus nidulans</i>	357.14	6.8	[72]
TTFB	415.7	2.0	Present study

and k_2) and correlation coefficient (R^2) were tabulated in Table 3. The kinetic sorption curves of the TTFB for CR adsorption is shown in Figure 4. The experimental ($q_{e, exp}$) and the calculated ($q_{e, cal}$) values from the PSO are very close to each other, and also, the estimated correlation coefficients, R^2 are even close or equal to 1 for PSO kinetics than that for the PFO kinetics. Therefore, the adsorption kinetics can be approximated more favorably by the PSO model than the PFO model for the adsorption of CR by TTFB. Similar adsorption kinetic behavior for banana peel,^[52] guava leaf-based activated carbon,^[53] and tea waste^[54] for CR has been reported.

Adsorption isotherms

To understand the adsorption behavior, the study of isothermal data is necessary. Many theoretical models could be applied to the experimental data for the best fit. Among which, the more common and familiar approaches of Langmuir, Freundlich, D-R, and Temkin nonlinear isotherm equations were used in the present study.

Langmuir isotherm^[55] is relevant in many adsorption processes. It based on the postulation that a monolayer of adsorbate formed on the external surface of the adsorbent and no further adsorption/layer after that. The Langmuir equation can be written in the following non-linear form:

$$q_e = \frac{q_{max}K_L C_e}{1 + K_L C_e} \quad (6)$$

The q_{max} for CR on TTFB was enhanced and raised from 318.1 to 415.7 mg/g (Table 2) with a rise in the temperature from 303 to 333 K, which could attribute to an increase in kinetic energy of the adsorbent particles due to the upsurge in temperature. The increase in dynamic energy raises the regularity of collisions between the sorbent and the sorbate, resulting in enhanced adsorption on to the surface of the adsorbent.^[56]

Freundlich model^[57] explains a heterogeneous (multilayer adsorption) adsorption system. The assumption of this model was that when the adsorbate concentration increases in the surrounding medium, leads to an increase in the deposition of the adsorbate concentration on the sorbent surface. The non-linear equation of the Freundlich isotherm

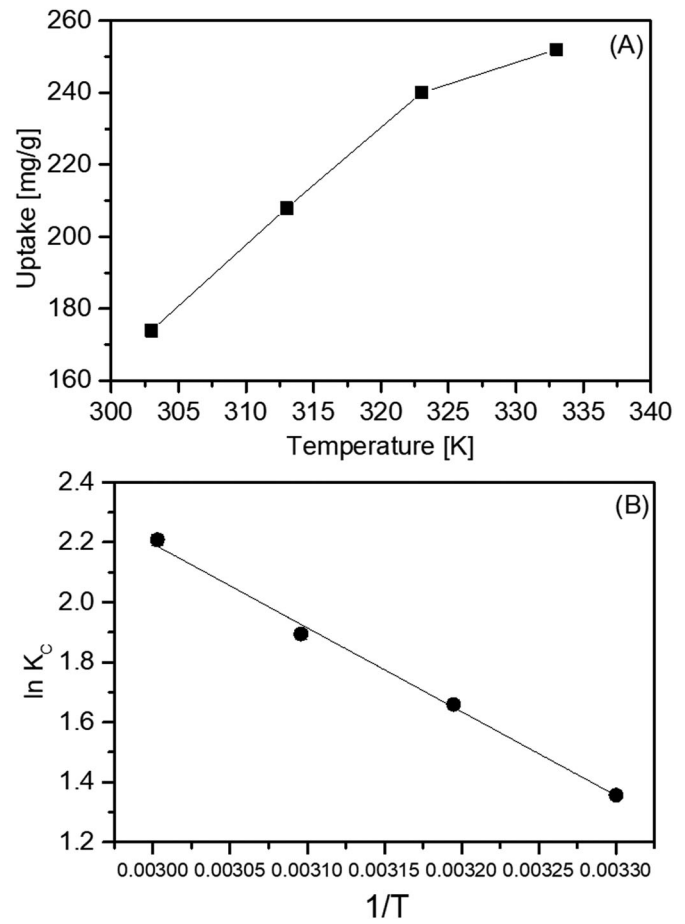


Figure 6. (A) Effect of temperature on the adsorption of CR onto TTFB and (B) Van't Hoff plot for the adsorption of CR onto TTFB.

model can be expressed as:

$$q_e = K_f C_e^{1/n} \quad (7)$$

The n value varies between 1.0 and 10.0 (i.e., $1/n < 1.0$), indicating that the adsorption of CR onto the TTFB was favorable at studied conditions. The n values that reflect the adsorption intensity also exposed the same trend. The n values (Table 2) obtained for the adsorption process represented favorable adsorption.

D-R isotherm^[58] signifies the role of the heterogeneous surface of the sorbent in the adsorption process. This model followed by high activities of solutes at moderate concentrations. The non-linear equation of D-R isotherm expressed by the following Eqs. (8) and (9):

$$q_e = q_m \exp(-K\varepsilon^2) \quad (8)$$

$$\varepsilon = RT \ln \left(1 + \frac{1}{C_e} \right) \quad (9)$$

The mean free energy of adsorption, E obtained from the following Eq. (10):

$$E = \frac{1}{\sqrt{2K}} \quad (10)$$

The magnitude of mean free energy E (kJ/mol) estimates the nature of the adsorption mechanism. Depending on the E value, i.e., < 8.0 kJ/mol, in between 8.0 and 16.0 kJ/mol,

Table 5. Thermodynamic parameters (ΔG° , ΔH° , and ΔS°) for the adsorption of CR onto TTFB.

Temp. (K)	ΔG° (kJ/mol)	ΔH° (kJ/mol)	ΔS° (kJ/mol K)
303	-3.4159		
313	-4.3186	23.2	0.088
323	-5.0864		
333	-6.1149		

and >16.0 kJ/mol, one can conclude that physical forces, chemical ion-exchange mechanism and particle diffusion respectively govern the process.^[59] The values of E (see Table 2) were lower than 8.0 kJ/mol, which suggested that the adsorption of CR onto TTFB involves the physisorption mechanism.

Temkin isotherm^[60] mainly considers the interactions of adsorbent-adsorbate, which is explained by a factor. When the adsorbent surface packed was with dye, there will be a linear decrease in the heat of the adsorption of all the molecules because of interactions. This theory mainly concerns that the decrease in heat of adsorption is linear and not logarithmic.

The nonlinear equation of Temkin isotherm expressed as:

$$q_e = \beta \ln \alpha + \beta \ln C_e \quad (11)$$

where $\beta = \frac{RT}{b}$

The value of b indicates either physisorption (<8.0 kJ/mol) or chemisorption (between 8.0 and 16.0 kJ/mol). Values of b (Table 2) in the present study was less than 8.0 kJ/mol, exhibited that the adsorption of CR onto TTFB is physisorption.

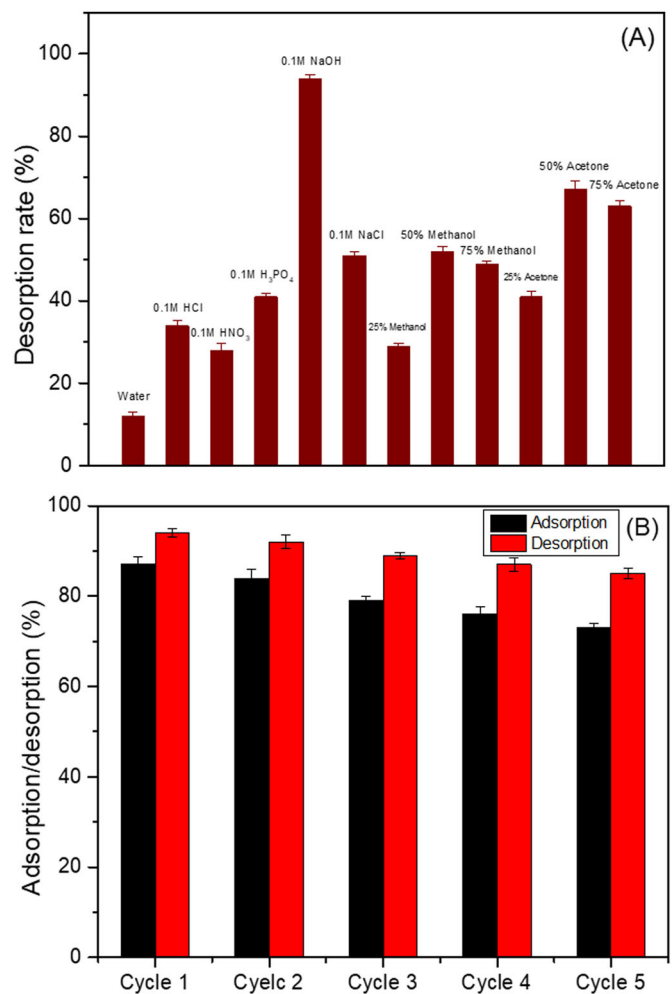
Figure 5 demonstrates the plots of the experimental and the predicted two-parameter isotherms (Langmuir, Freundlich, D-R, and Temkin) by nonlinear method for the adsorption of CR onto TTFB. All isotherm parameters, along with the correlation coefficients (R^2) and χ^2 values were tabulated in Table 2. Comparing these nonlinear isotherms, it is possible to identify the best-fitting adsorption isotherms; in lieu of the present study the order of exactness is as follows: Langmuir $>$ Temkin $>$ D-R $>$ Freundlich based on the association of higher R^2 (0.9961 – 0.9975) and lower χ^2 (31.3–61.7) values.

Comparison of TTFB with different adsorbents for CR removal

The maximum monolayer sorption capacities (q_{max}) of several adsorbents toward CR dye as reported literature^[61–72] was summarized in Table 4. A comparison between present work and other published data from the research shows that TTFB is an excellent adsorbent for CR compared to various adsorbents. Therefore, it could safely conclude that the TTFB has considerable potential for the removal of CR from an aqueous phase.

Effect of temperature

The temperature effect on the adsorption process of CR onto TTFB was shown in Figure 6A. The experiments were performed at four temperatures (303, 313, 323, and 333 K)

**Figure 7.** Desorption of CR using (A) different eluents and (B) 0.1 M NaOH after five adsorption-desorption cycles.

at a constant initial adsorbate concentration of 300 mg/L and a pH of 2.0. The experimental results exhibited that the sorption capacity increased with the rise in temperature. This indicates that the adsorption of CR onto TTFB is endothermic. The thermodynamic parameters involve Gibbs free energy change (ΔG°), entropy change (ΔS°), and enthalpy change (ΔH°), which are calculated by the following Eqs. (12–15), and the results listed in Table 5.

$$\Delta G^\circ = -RT \ln K_c \quad (12)$$

$$K_c = \frac{C_{Ae}}{C_e} \quad (13)$$

$$\Delta G^\circ = \Delta H^\circ - T\Delta S^\circ \quad (14)$$

$$\ln K_c = -\frac{\Delta G^\circ}{RT} = -\frac{\Delta H^\circ}{RT} + \frac{\Delta S^\circ}{R} \quad (15)$$

The values of ΔH° and ΔS° obtained from the slope and intercept of the plots of the layout of $\ln K_c$ according to $1/T$ (Figure 6B). The sign of ΔH° is positive means the reaction nature is endothermic during the adsorption process. The sign of ΔS° positive implies an increase in randomness at the junction of solid-liquid as a result of CR adsorption. The negative values of ΔG° at various temperatures (303–333 K) show that the adsorption is thermodynamically

feasible and is a spontaneous process. The decrease in ΔG° values with a rise in temperature suggested that the adsorption of CR was a favorable process because of its rapid dehydration at a higher temperature. The method concludes by the ΔG° values, such that when ΔG° values were > -20 kJ/mol, it is physisorption and lies between -80 and -400 kJ/mol, then it is chemisorption.^[73] In the present study, the values of ΔG° ranged between -3.4159 and -6.1149 kJ/mol. As a result, the adsorption process occurred as physisorption. Therefore, the adsorption process of CR by TTFB is a chemisorption driven physisorption. Electronic interactions initiated, supported and made the physical sorption process faster in the present study.

Desorption and regeneration evaluation

Desorption and regeneration experiments give useful insights about the possibility of the recovery of the adsorbent. Various desorbing eluents such as double distilled water, 0.1 M HCl, 0.1 M HNO₃, 0.1 M H₃PO₄, 0.1 M NaOH, 0.1 M NaCl, 25% methanol, 50% methanol, 75% methanol, 25% acetone, 50% acetone, and 75% acetone were used for the desorption experiments of CR-loaded TTFB to determine the best desorbing eluent. Figure 7A shows the desorption percentages of CR using various desorbing eluents. From the results, 0.1 M NaOH is the best eluent for the recovery of CR with 94% desorption among the other eluents. The regeneration experiments performed using 0.1 M NaOH. To determine the reusability of the adsorbent, five cycles were (adsorption-desorption) done using the same adsorbent. It can see from Figure 7B, nearly 94% of the adsorbed dye desorbed in the first cycle and then the desorbed dye amount decreased to 85% in the fifth cycle. The loss in the desorption efficiency of the TTFB for CR was found to be $< 9\%$. This may be because of the small loss of adsorbent during the adsorption-desorption process. The results showed that TTFB is an excellent reusable, economical and efficient sorbent, which can be successfully applied to remove CR from aqueous media.

Conclusions

The present study elucidates the effect of critical operational parameters such as solution pH, agitation speed, contact time, adsorbate concentration and temperature on the adsorption of CR using TTFB. FTIR, and SEM analysis asserted the presence of functional groups and surface morphology of the TTFB. The textural properties of TTFB show BET surface area, total pore volume, and mean pore diameter of 18.6 m²/g, 0.1126 cm³/g, and 23.2 nm, respectively. The pH_{pzc} of the TTFB was found to be 5.4. The maximum sorption capacities of CR onto TTFB were 318.1, 368.4, 394.8, and 415.7 mg/g at 303, 313, 323, and 333 K, respectively, observed at pH 2.0 and the adsorption process has reached equilibrium at 120 min. The sorption capacity increased with a rise in temperature of the solution indicating an endothermic process. The equilibrium non-linear isotherm models were used to reveal the adsorption data. Langmuir isotherm model is capable of representing the sorption data adequately than the other three

models (Freundlich, D-R, and Temkin). Adsorption kinetics of CR removal by TTFB follows the PSO model. Thermodynamic results (ΔG° , ΔS° , and ΔH°) showed that the adsorption of CR onto TTFB is spontaneous, feasible, and endothermic. Desorption experiments showed 94% recovery of CR with 0.1 M NaOH compared to the other eluents. Reusability of TTFB showed that after even five consecutive adsorption-desorption cycles, the desorption efficiency was 85%, which indicates that TTFB is a renewable adsorbent. Based on the results, TTFB can be used as an efficient low-cost sorbent for the removal of CR from the aqueous medium.

Nomenclature

<i>b</i>	Temkin constant (J/mol)
BET	Brunauer-Emmett-Teller
BJH	Barret-Joyner-Halenda
CR	congo red
<i>C_e</i>	equilibrium concentration in solution (mg/L)
<i>C_o</i>	initial concentration in the solution (mg/L)
<i>C_{Ae}</i>	solid phase concentration at equilibrium (mg/L)
D-R	Dubinin and Radushkevich
FTIR	Fourier Transform Infrared Spectroscopy
<i>k₁</i>	PFO rate constant (1/min)
<i>k₂</i>	PSO rate constant (g/mg min)
<i>K</i>	activity coefficient related to mean sorption energy (mol ² /J ²)
<i>K_c</i>	distribution constant
<i>K_f</i>	Freundlich constant (mg/g)
<i>K_L</i>	Langmuir constant (L/mg)
<i>M</i>	dry mass of adsorbent (g)
<i>n</i>	number of samples (χ^2 analysis)
<i>n</i>	the Freundlich intensity parameter (dimensionless)
<i>1/n</i>	heterogeneity factor
pH _{pzc}	point of zero charge
PFO	Pseudo-first-order
PSO	Pseudo-second-order
<i>q_e</i>	adsorbed value of CR at equilibrium concentration (mg/g)
<i>q_e</i>	experimental data of equilibrium capacity (mg/g) (χ^2 analysis)
<i>q_{e,m}</i>	equilibrium capacity (mg/g) obtained by calculating from model
<i>q_{e1}, q_{e2}</i>	amount of dye adsorbed at equilibrium (mg/g)
<i>q_t</i>	amount of dye adsorbed at time <i>t</i> (mg/g)
<i>q_{max}</i>	maximum monolayer coverage capacity (mg/g)
<i>q_m</i>	adsorption capacity (mg/g) (D-R model)
<i>R</i>	universal gas constant (8.314 kJ/mol K)
SEM	Scanning Electron Microscopy
<i>T</i>	absolute temperature (K)
<i>V</i>	volume of dye solution (L)
α	<i>Greek letters</i>
α	equilibrium binding constant (L/mg)
ε	Polanyi potential
χ^2	Chi-square

Funding

This work was financially supported by the Minister of Science and Technology (Project No: MOST 106-2625-M-224-002, MOST 106-2915-I-224-501, MOST 106-2625-M-224-002, MOST 107-2625-M-224-002, and MOST 108-2625-M-224-005), Taiwan.

References

- [1] Guo, D. D.; Li, B.; Deng, Z. P.; Huo, L. H.; Gao, S. Ladder Chain Cd-Based Polymer as a Highly Effective Adsorbent for

- Removal of Congo Red. *Ecotoxicol. Environ. Saf.* **2019**, *178*, 221–229. DOI: [10.1016/j.ecoenv.2019.04.042](https://doi.org/10.1016/j.ecoenv.2019.04.042).
- [2] Zhao, R.; Wang, Y.; Li, X.; Sun, B.; Wang, C. Synthesis of β -Cyclodextrin-Based Electrospun Nanofiber Membranes for Highly Efficient Adsorption and Separation of Methylene Blue. *ACS Appl. Mater. Interfaces* **2015**, *7*, 26649–26657. DOI: [10.1021/acsami.5b08403](https://doi.org/10.1021/acsami.5b08403).
- [3] Dâas, A.; Hamdaoui, O. Extraction of Anionic Dye from Aqueous Solutions by Emulsion Liquid Membrane. *J. Hazard. Mater.* **2010**, *178*, 973–981. DOI: [10.1016/j.jhazmat.2010.02.033](https://doi.org/10.1016/j.jhazmat.2010.02.033).
- [4] Shi, P.; Su, R.; Wan, F.; Zhu, M.; Li, D.; Xu, S. Co_3O_4 Nanocrystals on Graphene Oxide as a Synergistic Catalyst for Degradation of Orange II in Water by Advanced Oxidation Technology Based on Sulfate Radicals. *Appl. Catal. B Environ.* **2012**, *123–124*, 265–272. DOI: [10.1016/j.apcatb.2012.04.043](https://doi.org/10.1016/j.apcatb.2012.04.043).
- [5] Nipane, S. V.; Korake, P. V.; Gokavi, G. S. Graphene-Zinc Oxide Nanorod Nanocomposite as Photocatalyst for Enhanced Degradation of Dyes under UV Light Irradiation. *Ceram. Int.* **2015**, *41*, 4549–4557. DOI: [10.1016/j.ceramint.2014.11.151](https://doi.org/10.1016/j.ceramint.2014.11.151).
- [6] Sadri Moghaddam, S.; Alavi Moghaddam, M. R.; Arami, M. Coagulation/Flocculation Process for Dye Removal Using Sludge from Water Treatment Plant: Optimization through Response Surface Methodology. *J. Hazard. Mater.* **2010**, *175*, 651–657. DOI: [10.1016/j.jhazmat.2009.10.058](https://doi.org/10.1016/j.jhazmat.2009.10.058).
- [7] Hu, E.; Wu, X.; Shang, S.; Tao, X. M.; Jiang, S. X.; Gan, L. Catalytic Ozonation of Simulated Textile Dyeing Wastewater Using Mesoporous Carbon Aerogel Supported Copper Oxide Catalyst. *J. Clean. Prod.* **2016**, *112*, 4710–4718. DOI: [10.1016/j.jclepro.2015.06.127](https://doi.org/10.1016/j.jclepro.2015.06.127).
- [8] Liu, J.; Zhuo, Z.; Xie, W.; Kuo, J.; Lu, X.; Buyukada, M.; Evrendilek, F. Interaction Effects of Chlorine and Phosphorus on Thermochemical Behaviors of Heavy Metals during Incineration of Sulfur-Rich Textile Dyeing Sludge. *Chem. Eng. J.* **2018**, *351*, 897–911. DOI: [10.1016/j.cej.2018.06.158](https://doi.org/10.1016/j.cej.2018.06.158).
- [9] Munagapati, V. S.; Wen, J. C.; Pan, C. L.; Gutha, Y.; Wen, J. H. Enhanced Adsorption Performance of Reactive Red 120 Azo Dye from Aqueous Solution Using Quaternary Amine Modified Orange Peel Powder. *J. Mol. Liq.* **2019**, *285*, 375–385. DOI: [10.1016/j.molliq.2019.04.081](https://doi.org/10.1016/j.molliq.2019.04.081).
- [10] Al-Aoh, H. A.; Jamil Maah, M.; Ahmad, A. A.; Radzi Bin Abas, M. Adsorption of 4-Nitrophenol on Palm Oil Fuel Ash Activated by Amino Silane Coupling Agent. *Desalin. Water Treat.* **2012**, *40*, 159–167. DOI: [10.5004/dwt.2012.2841](https://doi.org/10.5004/dwt.2012.2841).
- [11] Al-Aoh, H. A.; Maah, M. J.; Yahya, R.; Bin Abas, M. R. Isotherms, Kinetics and Thermodynamics of 4-Nitrophenol Adsorption on Fiber-Based Activated Carbon from Coconut Husks Prepared under Optimized Conditions. *Asian J. Chem.* **2013**, *25*, 9573–9581. DOI: [10.14233/ajchem.2013.15082](https://doi.org/10.14233/ajchem.2013.15082).
- [12] Al-Aoh, H. A. Adsorption of MnO_4^- from a Aqueous Solution by *Nitraria retusa* Leaves Powder; Kinetic, Equilibrium and Thermodynamic Studies. *Mater. Res. Express* **2019**, *6*, 115102. DOI: [10.1088/2053-1591/ab4668](https://doi.org/10.1088/2053-1591/ab4668).
- [13] Al-Aoh, H. A. Equilibrium, Thermodynamic and Kinetic Study for Potassium Permanganate Adsorption by Neem Leaves Powder. *Desalin Water Treat.* **2019**, *170*, 101–110. DOI: [10.5004/dwt.2019.24905](https://doi.org/10.5004/dwt.2019.24905).
- [14] Kallel, F.; Bouaziz, F.; Chaari, F.; Belghith, L.; Ghorbel, R.; Chaabouni, S. E. Interactive Effect of Garlic Straw on the Sorption and Desorption of Direct Red 80 from Aqueous Solution. *Process Saf. Environ. Prot.* **2016**, *102*, 30–43. DOI: [10.1016/j.psep.2016.02.012](https://doi.org/10.1016/j.psep.2016.02.012).
- [15] Irem, S.; Mahmood Khan, Q.; Islam, E.; Jamal Hashmat, A.; Anwar Ul Haq, M.; Afzal, M.; Mustafa, T. Enhanced Removal of Reactive Navy Blue Dye Using Powdered Orange Waste. *Ecol. Eng.* **2013**, *58*, 399–405. DOI: [10.1016/j.ecoleng.2013.07.005](https://doi.org/10.1016/j.ecoleng.2013.07.005).
- [16] Singh, H.; Chauhan, G.; Jain, A. K.; Sharma, S. K. Adsorptive Potential of Agricultural Wastes for Removal of Dyes from Aqueous Solutions. *J. Environ. Chem. Eng.* **2017**, *5*, 122–135. DOI: [10.1016/j.jece.2016.11.030](https://doi.org/10.1016/j.jece.2016.11.030).
- [17] Sartape, A. S.; Mandhare, A. M.; Jadhav, V. V.; Raut, P. D.; Anuse, M. A.; Kolekar, S. S. Removal of Malachite Green Dye from Aqueous Solution with Adsorption Technique Using *Limonia Acidissima* (Wood Apple) Shell as Low Cost Adsorbent. *Arab. J. Chem.* **2017**, *10*, S3229–S3238. DOI: [10.1016/j.arabjc.2013.12.019](https://doi.org/10.1016/j.arabjc.2013.12.019).
- [18] Lim, L. B. L.; Priyantha, N.; Tennakoon, D. T. B.; Chieng, H. I.; Dahri, M. K.; Suklueng, M. Breadnut Peel as a Highly Effective Low-Cost Biosorbent for Methylene Blue: Equilibrium, Thermodynamic and Kinetic Studies. *Arab. J. Chem.* **2017**, *10*, S3216–S3228. DOI: [10.1016/j.arabjc.2013.12.018](https://doi.org/10.1016/j.arabjc.2013.12.018).
- [19] Saeed, A.; Sharif, M.; Iqbal, M. Application Potential of Grapefruit Peel as Dye Sorbent: Kinetics, Equilibrium and Mechanism of Crystal Violet Adsorption. *J. Hazard. Mater.* **2010**, *179*, 564–572. DOI: [10.1016/j.jhazmat.2010.03.041](https://doi.org/10.1016/j.jhazmat.2010.03.041).
- [20] Kamranifar, M.; Khodadadi, M.; Samiei, V.; Dehdashti, B.; Noori Sepehr, M.; Rafati, L.; Nasseh, N. Comparison the Removal of Reactive Red 195 Dye Using Powder and Ash of Barberry Stem as a Low Cost Adsorbent from Aqueous Solutions: Isotherm and Kinetic Study. *J. Mol. Liq.* **2018**, *255*, 572–577. DOI: [10.1016/j.molliq.2018.01.188](https://doi.org/10.1016/j.molliq.2018.01.188).
- [21] Khodabandehloo, A.; Rahbar-Kelishami, A.; Shayesteh, H. Methylene Blue Removal Using *Salix babylonica* (Weeping Willow) Leaves Powder as a Low-Cost Biosorbent in Batch Mode: Kinetic, Equilibrium, and Thermodynamic Studies. *J. Mol. Liq.* **2017**, *244*, 540–548. DOI: [10.1016/j.molliq.2017.08.108](https://doi.org/10.1016/j.molliq.2017.08.108).
- [22] Miyah, Y.; Lahrachi, A.; Idrissi, M.; Khalil, A.; Zerrouq, F. Adsorption of Methylene Blue Dye from Aqueous Solutions onto Walnut Shells Powder: Equilibrium and Kinetic Studies. *Surf. Interfaces* **2018**, *11*, 74–81. DOI: [10.1016/j.surfin.2018.03.006](https://doi.org/10.1016/j.surfin.2018.03.006).
- [23] McKay, G.; Porter, J. F.; Prasad, G. R. The Removal of Basic Dyes Aqueous Solution by Adsorption on Low-Cost Materials. *Water Air Soil Pollut.* **1999**, *114*, 423–438. [Mismatch] DOI: [10.1023/A:1005197308228](https://doi.org/10.1023/A:1005197308228).
- [24] Sun, G.; Xu, X. Sunflower Stalk as Adsorbents for Color Removal from Textile Wastewater. *Ind. Eng. Chem. Res.* **1997**, *36*, 808–812. DOI: [10.1021/ie9603833](https://doi.org/10.1021/ie9603833).
- [25] Gupta, V. K.; Srivastava, S. K.; Mohan, D. Equilibrium Uptake, Sorption Dynamics, Process Optimization, and Column Operations for the Removal and Recovery of Malachite Green from Wastewater Using Activated Carbon and Activated Slag. *Ind. Eng. Chem. Res.* **1997**, *36*, 2207–2218. DOI: [10.1021/ie960442c](https://doi.org/10.1021/ie960442c).
- [26] Al-Aoh, H. A.; Maah, M. J.; Yahya, R.; Bin Abas, M. R. Radzi Bin Abas, M. A Comparative Investigation on Adsorption Performances of Activated Carbon Prepared from Coconut Husk Fiber and Commercial Activated Carbon for Acid Red 27 Dye. *Asian J. Chem.* **2013**, *25*, 9582–9590. DOI: [10.14233/ajchem.2013.15082A](https://doi.org/10.14233/ajchem.2013.15082A).
- [27] Al-Aoh, H. A.; Yahya, R.; Jamil Maah, M.; Radzi Bin Abas, M. Adsorption of Methylene Blue on Activated Carbon Fiber Prepared from Coconut Husk: Isotherm, Kinetics and Thermodynamics Studies. *Desalin. Water Treat.* **2014**, *52*, 6720–6732. DOI: [10.1080/19443994.2013.831794](https://doi.org/10.1080/19443994.2013.831794).
- [28] Asma Omar, A.; Yahaya, A. H.; Yahya, R.; Al-Aoh, H. A. Isotherm Parameters of Methylene Blue Adsorption on Coconut Husk Fiber Based-Activated Carbon. *World App. Sci. J.* **2014**, *31*, 1–4. DOI: [10.5829/idosi.wasj.2014.31.arsem.1](https://doi.org/10.5829/idosi.wasj.2014.31.arsem.1).
- [29] Rangabhashiyam, S.; Nakkeeran, E.; Anu, N.; Selvaraju, N. Biosorption Potential of a Novel Powder, Prepared from *Ficus auriculata* Leaves, for Sequestration of Hexavalent Chromium from Aqueous Solutions. *Res. Chem. Intermed.* **2015**, *41*, 8405–8424. DOI: [10.1007/s11164-014-1900-6](https://doi.org/10.1007/s11164-014-1900-6).
- [30] Nakkeeran, E.; Rangabhashiyam, S.; Giri Nandagopal, M. S.; Selvaraju, N. Removal of Cr(VI) from Aqueous Solution Using *Strychnos Nux-Vomica* Shell as an Adsorbent. *Desalin. Water Treat.* **2016**, *57*, 23951–23964. DOI: [10.1080/19443994.2015.1137497](https://doi.org/10.1080/19443994.2015.1137497).

- [31] Nakkeeran, E.; Saranya, N.; Giri Nandagopal, M. S.; Santhiagu, A.; Selvaraju, N. Hexavalent Chromium Removal from Aqueous Solutions by a Novel Powder Prepared from Colocasia Esculenta Leaves. *Int. J. Phytoremediation*. **2016**, *18*, 812–821. DOI: [10.1080/15226514.2016.1146229](https://doi.org/10.1080/15226514.2016.1146229).
- [32] Rangabhashiyam, S.; Giri Nandagopal, M. S.; Nakkeeran, E.; Selvaraju, N. Adsorption of Hexavalent Chromium from Synthetic and Electroplating Effluent on Chemically Modified *Swietenia mahagoni* Shell in a Packed Bed Column. *Environ. Monit. Assess.* **2016**, *188*, 411. DOI: [10.1007/s10661-016-5415-z](https://doi.org/10.1007/s10661-016-5415-z).
- [33] Rashid, A.; Bhatti, H. N.; Iqbal, M.; Noreen, S. Fungal Biomass Composite with Bentonite for Nickel and Zinc Adsorption: A Mechanistic Study. *Ecol. Eng.* **2016**, *91*, 459–471. DOI: [10.1016/j.ecoleng.2016.03.014](https://doi.org/10.1016/j.ecoleng.2016.03.014).
- [34] Fan, H.; Yang, J. S.; Gao, T. G.; Yuan, H. L. Removal of a Low-Molecular Basic Dye (Azure Blue) from Aqueous Solutions by a Native Biomass of a Newly Isolated *Cladosporium* sp.: Kinetics, Equilibrium and Biosorption Simulation. *J. Taiwan Inst. Chem. Eng.* **2012**, *43*, 386–392. DOI: [10.1016/j.jtice.2011.11.001](https://doi.org/10.1016/j.jtice.2011.11.001).
- [35] Drumm, F. C.; Grassi, P.; Georgin, J.; Tonato, D.; Pfingsten Franco, D. S.; Chaves Neto, J. R.; Mazutti, M. A.; Jahn, S. L.; Dotto, G. L. Potentiality of the *Phoma* sp. Inactive Fungal Biomass, a Waste from the Bioherbicide Production, for the Treatment of Colored effluents. *Chemosphere* **2019**, *235*, 596–605. DOI: [10.1016/j.chemosphere.2019.06.169](https://doi.org/10.1016/j.chemosphere.2019.06.169).
- [36] Naskar, A.; Majumder, R. Understanding the Adsorption Behaviour of Acid Yellow 99 on *Aspergillus niger* Biomass. *J. Mol. Liq.* **2017**, *242*, 892–899. DOI: [10.1016/j.molliq.2017.05.155](https://doi.org/10.1016/j.molliq.2017.05.155).
- [37] Gajera, H. P.; Bambharolia, R. P.; Hirpara, D. G.; Patel, S. V.; Golakiya, B. A. Molecular Identification and Characterization of Novel *Hypocrea koningii* Associated with Azo Dyes Decolorization and Biodegradation of Textile Dye Effluents. *Process Saf. Environ. Prot.* **2015**, *98*, 406–416. DOI: [10.1016/j.psep.2015.10.005](https://doi.org/10.1016/j.psep.2015.10.005).
- [38] Khelifi, E.; Touhami, Y.; Bouallagui, H.; Hamdi, M. Biosorption of Indigo from Aqueous Solution by Dead Fungal Biomass *Aspergillus alliaceus*. *Desalin. Water Treat.* **2013**, *53*, 1–984. DOI: [10.1080/19443994850745](https://doi.org/10.1080/19443994850745).
- [39] Aytar, P.; Bozkurt, D.; Erol, S.; Özdemir, M.; Çabuk, A. Increased Removal of Reactive Blue 72 and 13 Acidic Textile Dyes by *Penicillium ochrochloron* Fungus Isolated from Acidic Mine Drainage. *Desalin. Water Treat.* **2016**, *57*, 19333–19343. DOI: [10.1080/19443994.2015.1098567](https://doi.org/10.1080/19443994.2015.1098567).
- [40] Kodal, S. P.; Aksu, Z. Cationic Surfactant-Modified Biosorption of Anionic Dyes by Dried *Rhizopus arrhizus*. *Environ. Technol.* **2017**, *38*, 2551–2561. DOI: [10.1080/09593330.2016.1270357](https://doi.org/10.1080/09593330.2016.1270357).
- [41] Caner, N.; Kiran, I.; Ilhan, S.; Pinarbasi, A.; Iscen, C. F. Biosorption of Reactive Yellow 145 Dye by Dried *Penicillium restrictum*: Isotherm, Kinetic, and Thermodynamic Studies. *Sep. Sci. Technol.* **2011**, *46*, 2283–2290. DOI: [10.1080/01496395.2011.585211](https://doi.org/10.1080/01496395.2011.585211).
- [42] Baskar, G.; Pavithra, S. K.; Sheraz Fahad, K.; Renganathan, S. Optimization, Equilibrium, Kinetic Modeling, and Thermodynamic Studies of Biosorption of Aniline Blue by the Dead Biomass of *Aspergillus fumigatus*. *Desalin. Water Treat.* **2014**, *52*, 3547–3554. DOI: [10.1080/19443994.2013.803654](https://doi.org/10.1080/19443994.2013.803654).
- [43] Oussalah, A.; Boukerroui, A.; Aichour, A.; Djellouli, B. Cationic and Anionic Dyes Removal by Low-Cost Hybrid Alginate/Natural Bentonite Composite Beads: Adsorption and Reusability Studies. *Int. J. Biol. Macromol.* **2019**, *124*, 854–862. DOI: [10.1016/j.ijbiomac.2018.11.197](https://doi.org/10.1016/j.ijbiomac.2018.11.197).
- [44] Jain, S. N.; Gogate, P. R. Efficient Removal of Acid Green 25 Dye from Wastewater Using Activated *Prunus Dulcis* as Biosorbent: Batch and Column Studies. *J. Environ. Manage.* **2018**, *210*, 226–238. DOI: [10.1016/j.jenvman.2018.01.008](https://doi.org/10.1016/j.jenvman.2018.01.008).
- [45] Shah, B. A.; Shah, A. V.; Mistry, C. B.; Tailor, R. V.; Patel, H. D. Surface Modified Bagasse Fly Ash Zeolites for Removal of Reactive Black-5. *J. Dispers. Sci. Technol.* **2011**, *32*, 1247–1255. DOI: [10.1080/01932691.2010.505550](https://doi.org/10.1080/01932691.2010.505550).
- [46] Krika, F.; Benlahbib, O. F. Removal of Methyl Orange from Aqueous Solution via Adsorption on Cork as a Natural and Low-Coast Adsorbent: Equilibrium, Kinetic and Thermodynamic Study of Removal Process. *Desalin. Water Treat.* **2015**, *53*, 3711–3723. DOI: [10.1080/19443994.2014.995136](https://doi.org/10.1080/19443994.2014.995136).
- [47] Senthil Kumar, P.; Ramalingam, S.; Senthamarai, C.; Niranjanaa, M.; Vijayalakshmi, P.; Sivanesan, S. Adsorption of Dye from Aqueous Solution by Cashew Nut Shell: Studies on Equilibrium Isotherm, Kinetics and Thermodynamics of Interactions. *Desalination* **2010**, *261*, 52–60. DOI: [10.1016/j.desal.2010.05.032](https://doi.org/10.1016/j.desal.2010.05.032).
- [48] da Silva, L. G.; Ruggiero, R.; Gontijo, P.; de, M.; Pinto, R. B.; Royer, B.; Lima, E. C.; Fernandes, T. H. M.; Calvete, T. Adsorption of Brilliant Red 2BE Dye from Water Solutions by a Chemically Modified Sugarcane Bagasse Lignin. *Chem. Eng. J.* **2011**, *168*, 620–628. DOI: [10.1016/j.cej.2011.01.040](https://doi.org/10.1016/j.cej.2011.01.040).
- [49] Cardoso, N. F.; Lima, E. C.; Calvete, T.; Pinto, I. S.; Amavisca, C. V.; Fernandes, T. H. M.; Pinto, R. B.; Alencar, W. S. Application of Acai Stalks as Biosorbents for the Removal of the Dyes Reactive Black 5 and Reactive Orange 16 from Aqueous Solution. *J. Chem. Eng. Data* **2011**, *56*, 1857–1868. DOI: [10.1021/je100866c](https://doi.org/10.1021/je100866c).
- [50] Lagergren, S. About the Theory of So-Called Adsorption of Soluble Substances. *K. Sven. Vetenskapsakad. Handl.* **1898**, *24*, 1–39.
- [51] Ho, Y. S.; McKay, G. Pseudo-Second Order Model for Sorption Processes. *Process Biochem.* **1999**, *34*, 451–465. DOI: [10.1016/S0032-9592\(98\)00112-5](https://doi.org/10.1016/S0032-9592(98)00112-5).
- [52] Mondal, N. K.; Kar, S. Potentiality of Banana Peel for Removal of Congo Red Dye from Aqueous Solution: Isotherm, Kinetics and Thermodynamics. *Appl. Water Sci.* **2018**, *8*, 157. DOI: [10.1007/s13201-018-0811-x](https://doi.org/10.1007/s13201-018-0811-x).
- [53] Ojedokun, A. T.; Bello, O. S. Kinetic Modeling of Liquid-Phase Adsorption of Congo Red Dye Using Guava Leaf-Based Activated Carbon. *Appl. Water Sci.* **2017**, *7*, 1965–1977. DOI: [10.1007/s13201-015-0375-y](https://doi.org/10.1007/s13201-015-0375-y).
- [54] Foroughi-Dahr, M.; Abolghasemi, H.; Esmaili, M.; Shojamoradi, A.; Fatoorehchi, H. Adsorption Characteristics of Congo Red from Aqueous Solution onto Tea Waste. *Chem. Eng. Commun.* **2015**, *202*, 181–193. DOI: [10.1080/00986445.2013.836633](https://doi.org/10.1080/00986445.2013.836633).
- [55] Langmuir, I. The Adsorption of Gases on Plane Surfaces of Glass, Mica and Platinum. *J. Am. Chem. Soc.* **1918**, *40*, 1361–1403. DOI: [10.1021/ja02242a004](https://doi.org/10.1021/ja02242a004).
- [56] Harikishore Kumar Reddy, D.; Harinath, Y.; Seshaiha, K.; Reddy, A. V. R. Biosorption of Pb(II) from Aqueous Solutions Using Chemically Modified *Moringa oleifera* Tree Leaves. *Chem. Eng. J.* **2010**, *162*, 626–634. DOI: [10.1016/j.cej.2010.06.010](https://doi.org/10.1016/j.cej.2010.06.010).
- [57] Freundlich, H. M. F. Über Die Adsorption in Lasugen. *J. Phys. Chem.* **1906**, *57*, 385–470.
- [58] Dubinin, M. M. The Potential Theory of Adsorption of Gases and Vapors for Adsorbents with Energetically Non-Uniform Surface. *Chem. Rev.* **1960**, *60*, 235–266. DOI: [10.1021/cr60204a006](https://doi.org/10.1021/cr60204a006).
- [59] Chen, S.; Qin, C.; Wang, T.; Chen, F.; Li, X.; Hou, H.; Zhou, M. Study on the Adsorption of Dyestuffs with Different Properties by Sludge-Rice Husk Biochar: Adsorption Capacity, Isotherm, Kinetic, Thermodynamics and Mechanism. *J. Mol. Liq.* **2019**, *285*, 62–74. DOI: [10.1016/j.molliq.2019.04.035](https://doi.org/10.1016/j.molliq.2019.04.035).
- [60] Temkin, M. I.; Pyzhev, V. Kinetics of Ammonia Synthesis on Promoted Iron Catalysts. *Acta Physicochim. URSS* **1940**, *12*, 327–356.
- [61] Tian, X.; Li, C.; Yang, H.; Ye, Z.; Xu, H. Spent Mushroom: A New Low-Cost Adsorbent for Removal of Congo Red from Aqueous Solutions. *Desalin. Water Treat.* **2011**, *27*, 319–326. DOI: [10.5004/dwt.2011.2152](https://doi.org/10.5004/dwt.2011.2152).
- [62] Bouras, H. D.; Yeddou, A. R.; Bouras, N.; Hellel, D.; Holtz, M. D.; Sabaou, N.; Chergui, A.; Nadjemi, B. Biosorption of Congo Red Dye by *Aspergillus carbonarius* M333 and

- Penicillium glabrum* Pgl: Kinetics, Equilibrium and Thermodynamic Studies. *J. Taiwan Inst. Chem. Eng.* **2017**, *80*, 915–923. DOI: [10.1016/j.jtice.2017.08.002](https://doi.org/10.1016/j.jtice.2017.08.002).
- [63] Wang, M. X.; Zhang, Q. L.; Yao, S. J. A Novel Biosorbent Formed of Marine-Derived *Penicillium janthinellum* Mycelial Pellets for Removing Dyes from Dye-Containing Wastewater. *Chem. Eng. J.* **2015**, *259*, 837–844. DOI: [10.1016/j.ccej.2014.08.003](https://doi.org/10.1016/j.ccej.2014.08.003).
- [64] Zhang, Z.; Moghaddam, L.; O'Hara, I. M.; Doherty, W. O. S. Congo Red Adsorption by Ball-Milled Sugarcane Bagasse. *Chem. Eng. J.* **2011**, *178*, 122–128. DOI: [10.1016/j.ccej.2011.10.024](https://doi.org/10.1016/j.ccej.2011.10.024).
- [65] Vieira, S. S.; Magriotis, Z. M.; Santos, N. A. V.; Cardoso, M.; das, G.; Saczk, A. A. Macauba Palm (*Acrocomia aculeata*) Cake from Biodiesel Processing: An Efficient and Low Cost Substrate for the Adsorption of Dyes. *Chem. Eng. J.* **2012**, *183*, 152–161. DOI: [10.1016/j.ccej.2011.12.047](https://doi.org/10.1016/j.ccej.2011.12.047).
- [66] Munagapati, V. S.; Yarramuthi, V.; Kim, Y.; Lee, K. M.; Kim, D. S. Removal of Anionic Dyes (Reactive Black 5 and Congo Red) from Aqueous Solutions Using Banana Peel Powder as an Adsorbent. *Ecotoxicol. Environ. Saf.* **2018**, *148*, 601–607. DOI: [10.1016/j.ecoenv.2017.10.075](https://doi.org/10.1016/j.ecoenv.2017.10.075).
- [67] Somasekhara Reddy, M. C.; Sivaramakrishna, L.; Varada Reddy, A. The Use of an Agricultural Waste Material, Jujuba Seeds for the Removal of Anionic Dye (Congo Red) from Aqueous Medium. *J. Hazard. Mater.* **2012**, *203–204*, 118–127. DOI: [10.1016/j.jhazmat.2011.11.083](https://doi.org/10.1016/j.jhazmat.2011.11.083).
- [68] Ojedokun, A. T.; Bello, O. S. Liquid Phase Adsorption of Congo Red Dye on Functionalized Corn Cobs. *J. Dispers. Sci. Technol.* **2017**, *38*, 1285–1294. DOI: [10.1080/01932691.2016.1234384](https://doi.org/10.1080/01932691.2016.1234384).
- [69] Hu, Z.; Chen, H.; Ji, F.; Yuan, S. Removal of Congo Red from Aqueous Solution by Cattail Root. *J. Hazard. Mater.* **2010**, *173*, 292–297. DOI: [10.1016/j.jhazmat.2009.08.082](https://doi.org/10.1016/j.jhazmat.2009.08.082).
- [70] Yang, Y.; Wang, G.; Wang, B.; Li, Z.; Jia, X.; Zhou, Q.; Zhao, Y. Biosorption of Acid Black 172 and Congo Red from Aqueous Solution by Nonviable *Penicillium YW 01*: Kinetic Study, Equilibrium Isotherm and Artificial Neural Network Modeling. *Bioresour. Technol.* **2011**, *102*, 828–834. DOI: [10.1016/j.biortech.2010.08.125](https://doi.org/10.1016/j.biortech.2010.08.125).
- [71] Pathania, D.; Sharma, A.; Siddiqi, Z. M. Removal of Congo Red Dye from Aqueous System Using *Phoenix dactylifera* Seeds. *J. Mol. Liq.* **2016**, *219*, 359–367. DOI: [10.1016/j.molliq.2016.03.020](https://doi.org/10.1016/j.molliq.2016.03.020).
- [72] Xi, Y.; Shen, Y. F.; Yang, F.; Yang, G. J.; Liu, C.; Zhang, Z.; Zhu, D. H. Removal of Azo Dye from Aqueous Solution by a New Biosorbent Prepared with *Aspergillus nidulans* Cultured in Tobacco Wastewater. *J. Taiwan Inst. Chem. Eng.* **2013**, *44*, 815–820. DOI: [10.1016/j.jtice.2013.01.031](https://doi.org/10.1016/j.jtice.2013.01.031).
- [73] Gündüz, F.; Bayrak, B. Biosorption of Malachite Green from an Aqueous Solution Using Pomegranate Peel: Equilibrium Modelling, Kinetic and Thermodynamic Studies. *J. Mol. Liq.* **2017**, *243*, 790–798. DOI: [10.1016/j.molliq.2017.08.095](https://doi.org/10.1016/j.molliq.2017.08.095).